

OPTIMIZING THE FABRICATION PROCESS FOR SUPERIOR MECHANICAL PROPERTIES IN THE STOICHIOMETRIC SiC FIBER REINFORCED FCVI SiC MATRIX COMPOSITE SYSTEM

T. Taguchi^a, N. Igawa^a, T. Nozawa^b, K. Hironaka^b, L. L. Snead^c, T. Hinoki^c, Y. Katoh^b, S. Jitsukawa^a, A. Kohyama^b and J. C. McLaughlin^c

^a Japan Atomic Energy Research Institute, Tokai, Ibaraki 319-1195, Japan

^b Kyoto University, Gokasho, Uji, Kyoto 611-0011, Japan

^c Oak Ridge National Laboratory, P.O. Box 2008, Oak Ridge, TN 37831, USA

Objective

The purpose of this work is the fabrication of the 300 mm diameter SiC/SiC composite using new stoichiometric SiC fibers, such as Tyranno SA and Hi-Nicalon Type S fiber, of low porosity and high tensile strength. Before these large size composite are fabricated, the fabrication process of smaller size (75 mm diameter) SiC/SiC composite using the new SiC fibers by FCVI process required optimization. In addition, the effect of the interphase between fiber and matrix on the mechanical properties of composites was also investigated

Summary

Optimization of the fabrication for SiC composites with stoichiometric SiC fibers (Hi-Nicalon Type S and Tyranno SA) by the forced thermal-gradient chemical vapor infiltration (FCVI) process was carried out. Density and mechanical properties were improved by increasing the fiber volume fraction and optimizing precursor gas flow rates. Porosity was decreased to approximately 15%. Uniformity of fiber/matrix interphase was improved by changing the upstream side and downstream side of a preform during deposition. The tensile strength was seen to slightly increase with thickness of carbon interphase in the range of 75-300 nm. From these results, a dense 300 mm diameter SiC/SiC composite using Nicalon fiber as a trial experiment was fabricated. The density and porosity were 2.57 g/cm³ and 13.8 %, respectively.

Progress and status

1. Introduction

Ceramic matrix composites show excellent mechanical properties at high temperature and non-catastrophic failure behavior. These materials are therefore attractive candidates for structural applications at high temperature. For these reasons and their low residual radioactivity following the neutron irradiation, the continuous SiC-fiber reinforced SiC-matrix (SiC/SiC) composites are being actively investigated for first wall and blanket components in power fusion reactors [1-4].

Among the various fabrication processes, the chemical vapor infiltration (CVI) is one of the best techniques to fabricate the SiC/SiC because of the high purity and minimal fibers damage during the composite fabrication[5]. Whereas the isothermal CVI (I-CVI) can efficiently produce thin-wall and complex shape parts, it requires a significantly long time to produce thicker-wall materials. It takes high cost to produce the thick-wall materials by I-CVI. On the other hand, the forced-thermal gradient CVI (FCVI) of thicker parts can be effected at sufficiently high rates to only require tens of hours or less[5]. It can improve the cost to produce thick parts. We, therefore, adopted the FCVI process to make SiC/SiC composites in this study.

The large size composite is required to perform the variant thermal and mechanical properties for the both of un-irradiated and neutron irradiated specimens at the almost same microstructural property in each specimen, which includes the interphase structure and porosity. It is, therefore, very important

to fabricate the large size SiC/SiC composite with the uniform microstructural property. The definitive purpose in this study is the fabrication of the 300 mm diameter size SiC/SiC composite with the uniform microstructural properties.

Recently, high crystalline and stoichiometric SiC fibers have been produced including Hi-Nicalon Type S[6] and Tyranno SA[7], which possess superior mechanical and thermal properties as well as superior performance under neutron irradiation compared with their SiC-based predecessors. Because the properties of these advanced fibers, e.g. thermal conductivity, waviness, tensile modulus and fiber diameter, are very different from their predecessors, optimization of composite fabrication and interphase should be now being focused on their application. Before the 300 mm diameter size composite will be fabricated, it is important to optimize the fabrication process and the interphase by making the smaller size composite (75 mm diameter) in order to economize the cost. This study has also included general process optimization of properties such as through-thickness densification and interphase uniformity.

We adopted two kinds of advanced SiC fabrics as preforms: 2D-plain weave Tyranno SA and Hi-Nicalon Type S. Boron Nitride shows the excellent interphase for mechanical properties. Boron Nitride, however, is undesirable for fusion applications because nitrogen transmutes into ^{14}C that has a very long half-life of beta emitter by fusion neutrons, and also boron simultaneously produces helium and enhances radiation damage through recoil interaction. Therefore, the fusion community has limited the potential interphase materials to carbon, porous-SiC and multilayer-carbon/SiC are being studied for fusion applications [8]. Carbon interphase were selected for this study in the thickness range from 75 nm to 300 nm. Room temperature tensile properties were measured and optical and SEM observations of cross-sections and fracture surfaces in SiC/SiC were carried out in order to evaluate the thickness of interphase layer and investigate the effect of interphase on the mechanical properties of the composites.

2. Experimental procedure

Two kinds of advanced SiC fabric as preforms was adopted: 2D-plain Tyranno SA (Ube Industries, Ube, Japan) and Hi-Nicalon Type S (Nippon Carbon Co., Ltd., Tokyo, Japan).

The precursor for carbon deposition was 99% purity propylene (C_3H_6 , Matheson, Morrow, GA, USA)

Table 1. Fiber fabrics information of FCVI SiC/SiC composites

Specimen ID	Fiber	Weave type	Fiber orientation	Number of layers	Fiber as a spacer	Number of spacer layers
CVI1256	Tyranno SA	plane weave	[-30/0/+30]	55	P/W Nicalon	11
CVI1257	Hi-Nicalon Type S	plane weave	[-30/0/+30]	55	P/W Nicalon	8
CVI1258	Hi-Nicalon Type S	plane weave	[-30/0/+30]	45	P/W Nicalon	20
CVI1259	Hi-Nicalon Type S	plane weave	[-30/0/+30]	45	P/W Nicalon	20
CVI1260	Tyranno SA	plane weave	[-30/0/+30]	55	Tyranno SA grade 1	11
CVI1261	Tyranno SA	plane weave	[-30/0/+30]	58	Tyranno SA grade 1	13
CVI1264	Tyranno SA	plane weave	[0/90]	60	P/W Nicalon	11
CVI1265	Tyranno SA	plane weave	[0/90]	60	P/W Nicalon	11
CVI1266	Tyranno SA	plane weave	[0/90]	60	P/W Nicalon	11

and for SiC infiltration, technical grade methyltrichlorosilane (MTS, CH_3SiCl_3 , Gelest Inc., Tullytown, PA, USA) was used.

Table 2. Fabrication parameter of interphase

Specimen ID	Interface material	Thickness / nm	Source of interphase		Carrier gas		Temperature / C	Time / min
			Nominal	Material	Flow rate / cm^3/min	Material		
CVI1256	carbon	150	C_3H_6	50	Ar	1.0	1100	60
CVI1257	carbon	150	C_3H_6	50	Ar	1.0	1100	30+30
CVI1258	carbon	75	C_3H_6	50	Ar	1.0	1100	15+15
CVI1259	carbon	300	C_3H_6	50	Ar	1.0	1100	60+60
CVI1260	carbon	300	C_3H_6	50	Ar	1.0	1100	60+60
CVI1261	carbon	75	C_3H_6	50	Ar	1.0	1100	15+15
CVI1264	carbon	150	C_3H_6	50	Ar	1.0	1100	40+40
CVI1265	carbon	300	C_3H_6	50	Ar	1.0	1100	90+90
CVI1266	carbon	75	C_3H_6	50	Ar	1.0	1100	15+15

Table 3. fabrication parameters of F-CVI process

Specimen ID	Source of material		Carrier gas		Temperature / C	Run time / hours
	Material	Flow rate / g/min	Material	Flow rate / dm^3/min		
CVI1256	MTS	0.5	H_2	0.75	1200	66
CVI1257	MTS	0.5	H_2	0.75	1200	31
CVI1258	MTS	0.5 0.33	H_2	0.75 0.75	1200	21.5 3.5
CVI1259	MTS	0.5 0.33	H_2	0.75 0.75	1100	25.9 4.5
CVI1260	MTS	0.5 0.17	H_2	0.75 0.35	1200	16 6
CVI1261	MTS	0.17	H_2	0.35	1200	66
CVI1264	MTS	0.3	H_2	0.45	1100	61.5
CVI1265	MTS	0.3	H_2	0.45	1050	70.5
CVI1266	MTS	0.3	H_2	0.45	1000	90.2

The SiC fabric layers with a fabric layer orientation of $[-30^\circ/0^\circ/30^\circ]$ or $[0^\circ/90^\circ]$ were restrained in a graphite fixture. The fiber volume fraction range was 30 to 39 vol%. The size of preform was 75 mm in diameter and 12.5 mm thickness. The fiber fabric parameters of the fabricated SiC/SiC in this study are shown in Table 1. The carbon interphase was deposited at 1100°C and at 5 Pa. The condition of carbon deposition is flow rates of $50\text{ cm}^3/\text{min}$ C_3H_6 and $1000\text{ cm}^3/\text{min}$ Ar. The fabrication parameters of the interphases are shown in Table 2. After the interphase layer was deposited, the preforms were infiltrated at $1000\text{--}1200^\circ\text{C}$ at atmospheric pressure with MTS flow rate of $0.2\text{--}0.5\text{ g}/\text{min}$ carried by $450\text{--}750\text{ cm}^3/\text{min}$ of H_2 . The back-pressure was monitored and the FCVI process was automatically finished after the back pressure reached 6.9×10^4 Pa. The infiltration conditions are shown in Table 3.

To determine the distribution of porosity and carbon interphase thickness, the plate was cut into nine sections as shown in Fig. 2. The density of each section was calculated from the dimensions and the mass of the plate to determine the distribution of the porosity in the composite. The microstructure of the composites was observed by optical microscopy and scanning electron microscopy (SEM).

Tensile testing was carried out at room temperature with a cross-head speed of $0.5\text{ mm}/\text{min}$. The

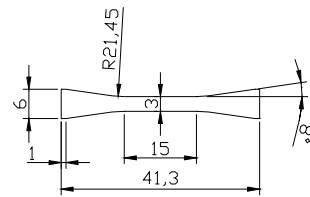


Fig. 1 Schematic illustration of tensile test specimen

shape and size of the specimen was shown in Fig. 1. The strain of the specimen was measured with bonded strain gauges. The fracture surfaces were observed by SEM in order to investigate the effect of interphase on the mechanical properties.

3. Results and discussion

3.1 Fabrication of the 75 mm diameter composite

3.1.1 Densification process

The distributions of the porosity in the fabricated SiC/SiC in this study are shown in Fig. 2. The characterization of SiC/SiC is also shown Table 4. The porosity in the ID 1257 specimen was relatively large (23.5 %) and depending on position: we found that the lower and outer position in the composite had the highest porosity. Much better uniform porosity in the composites (for example ID 1259 specimen) was obtained by decreasing the MTS and H₂ gas flow rates at the latter part of the FCVI process. Presently, the porosity in the composite was decreased. Because the termination of the FCVI process was controlled by the back-pressure that was decreased with decreasing the gas flow rate, the FCVI process was extended by the decrease in the flow rate.

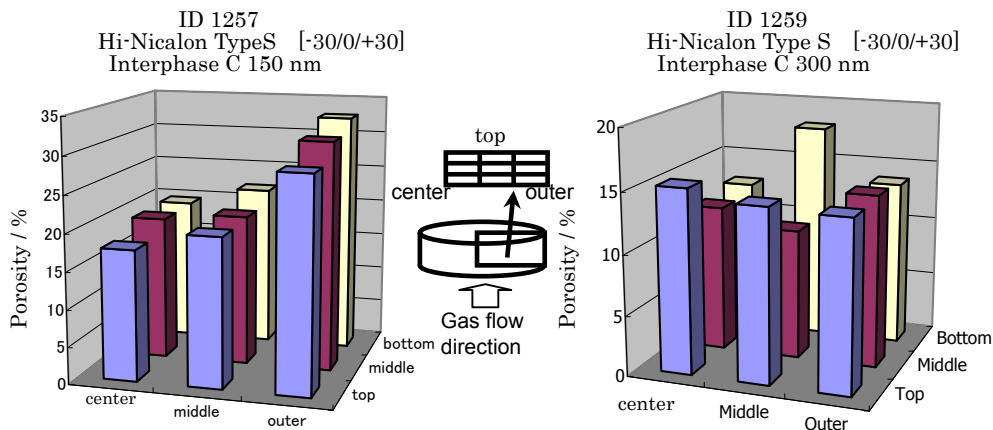


Fig.2 Typical distribution of the porosity of the fabricated SiC/SiC composite.

Table 4. Characterization of F-CVI SiC/SiC composites

Specimen ID	Fiber volume fraction / %	Density / g/cm ³	Porosity / %
CVI1256	37.0	2.67 ± 0.12	15.1 ± 4.0
CVI1257	33.0	2.43 ± 0.18	23.5 ± 5.7
CVI1258	36.1	-----	-----
CVI1259	35.0	2.73 ± 0.07	13.9 ± 2.1
CVI1260	30.2	2.41 ± 0.09	24.2 ± 2.8
CVI1261	33.3	2.53 ± 0.13	20.4 ± 4.2
CVI1264	35.4	2.43 ± 0.12	23.3 ± 3.7
CVI1265	35.3	2.60 ± 0.14	18.0 ± 4.5
CVI1266	35.2	2.60 ± 0.17	18.1 ± 5.3

The average porosity as a function of fiber volume fraction was shown in Fig. 3. The fiber volume fraction is very effective in decreasing the porosity; the average porosity is decreased to 15 % by increasing the fiber volume fraction to 39 vol%, but seems independence of fiber type and infiltration parameter.

The typical cross-sections of SiC/SiC are shown in Fig. 4. Even in the specimen that had smallest porosity (15.1 %), we could observe the two kinds of pores; the one is the inter-bundle large pores and

the another is the intra-bundle small pores. The porosity in the composite depends on the amount of inter-bundle pore more efficiently than that of intra-bundle pore because the total amount of inter-bundle pore is much larger than that of intra-bundle pore. From the cross-sections microphotographs, it was found that the size of inter-bundle pores was smaller with the shorter distance between the fiber bundles in the specimen. The distance between fiber bundles is shorter when fiber volume fraction is higher, which mean each space between bundles with higher fiber volume fraction is smaller than those with lower fiber volume fraction; therefore the size of inter-bundle pore at higher fiber volume fractions is smaller than those of lower fiber volume fraction.

3.1.2 Interphase fabrication process

Figure 5 shows the distribution of the thickness of carbon interphase between SiC fiber and SiC matrix in the composites estimated from cross-section SEM images. The results of the thickness of carbon are shown in Table. 5. In ID1256 specimen, we found that the lower position in the composite had the thicker carbon interphase: the average thickness of carbon interphase at bottom is about 145 nm whereas that

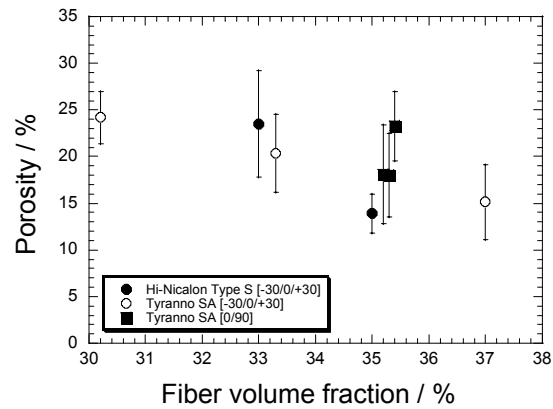


Fig.3 Effect of fiber volume fraction on the porosity.

ID 1256 Porosity 15.1 % ID 1260 Porosity 24.2 %

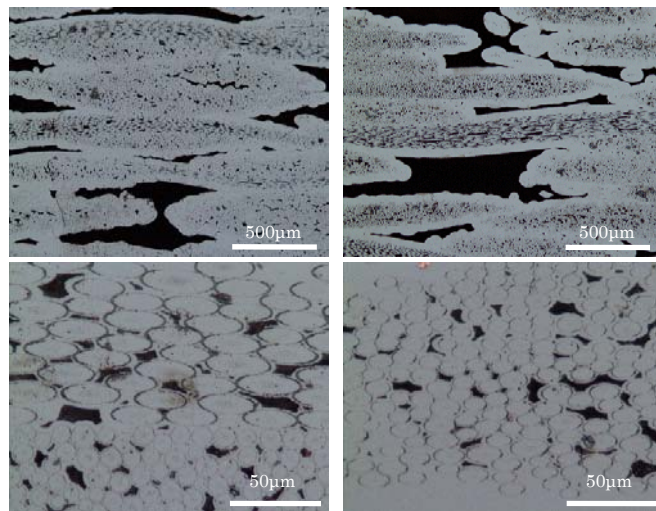


Fig.4 Cross-sections photographs of SiC/SiC composites.

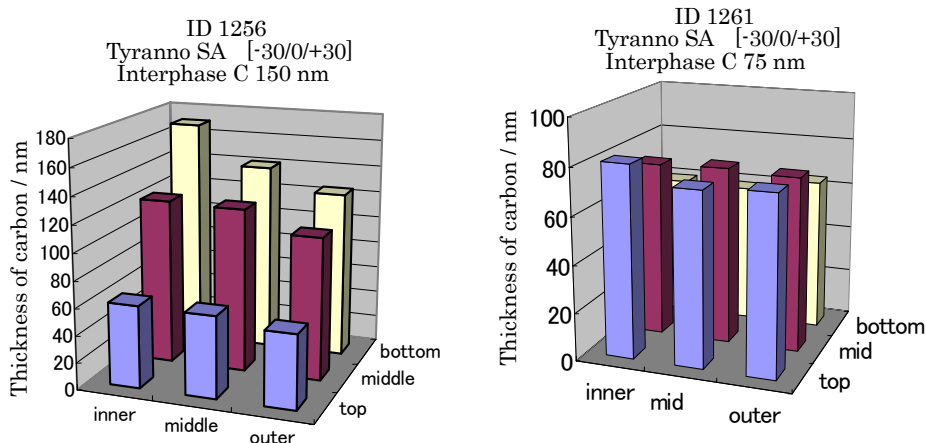


Fig.5 Typical distribution of the carbon thickness in the SiC/SiC composite

at top 60 nm. This tendency was attributed to a concentration gradient in the C_3H_6 gas. This material gas traveled from the bottom surface to top of the specimen, and the thickness of specimen was so large that the concentration of C_3H_6 gas was decreased due to its consumption at the lower part of the specimen. To mitigate this problem the preform was flipped midway through the interphase infiltration. The distribution of carbon interphase thickness was remarkably improved and we obtained the specimens with near uniform through-thickness carbon interphase thickness (see ID1261 specimen in Fig.5).

Table 5. Interphase thickness of F-CVI SiC/SiC composites

Specimen ID	material	Thickness of interphase / nm				
		nominal	Measured average	Minimum	Maximum	Statistical scatter
CVI1256	carbon	150	107.1	54.8	170.1	40.1
CVI1257	carbon	150	159.5	141.9	172.7	10.8
CVI1258	carbon	75	-----	-----	-----	-----
CVI1259	carbon	300	407.3	266.4	612.2	121.3
CVI1260	carbon	300	168.5	138.2	206.9	22.1
CVI1261	carbon	75	70.5	58.8	81.1	7.8
CVI1264	carbon	150	116.4	86.1	154.5	20.5
CVI1265	carbon	300	225.5	168.0	256.3	29.4
CVI1266	carbon	75	42.3	28.5	54.2	7.2

The relationship between the average thickness of carbon interphase and deposition time is shown in Fig.6. The thickness of carbon interphase increased linearly with increasing the deposition time. The carbon deposition rate of the composite using Hi-Nicalon Type S fiber is, however, larger than that of the composite using Tyranno SA fiber. In the case of the same fiber volume fraction, the total superficies of fibers of the composite using Hi-Nicalon Type S is smaller than that of the composite using Tyranno SA fiber because the diameter of Hi-Nicalon Type S fiber is larger than that of Tyranno SA fiber. It is, therefore, considered that the carbon deposition rate of the composite using Hi-Nicalon Type S was larger than that of the composite using Tyranno SA. The relationship between the thickness of carbon and the standardized deposition time (the deposition time divided by the total superficies of fibers) is shown in Fig.7. The average thickness of carbon in all composites increased as one linear series with increasing the standardized deposition time. Therefore we can estimate the carbon thickness from the standardized deposition time, even if any kinds of fiber are used in the

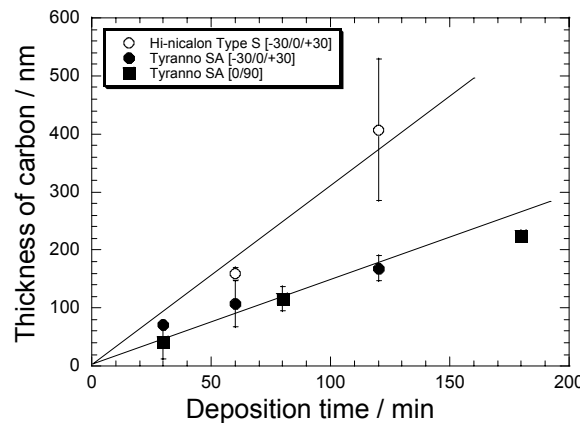


Fig.6 Relationship between deposition time and carbon thickness.

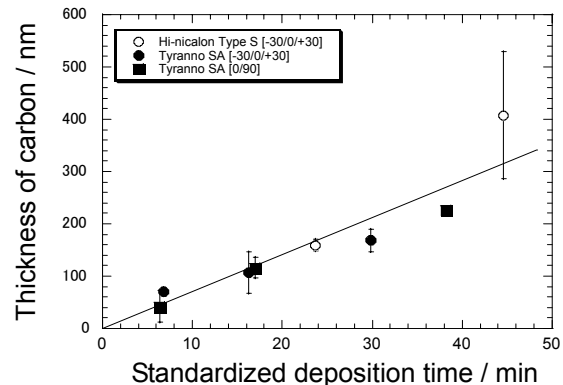


Fig.7 Relationship between standardized deposition time and carbon thickness.

composite.

3.1.3 Mechanical properties

Typical stress-strain curves during the tensile testing are seen in Fig. 8. The summaries of tensile strength testing in the composites with carbon layer as the interphase layer are shown in Table 6. In tensile testing, each specimen exhibited nonlinear stress-strain behavior, which means noncatastrophic failure behavior.

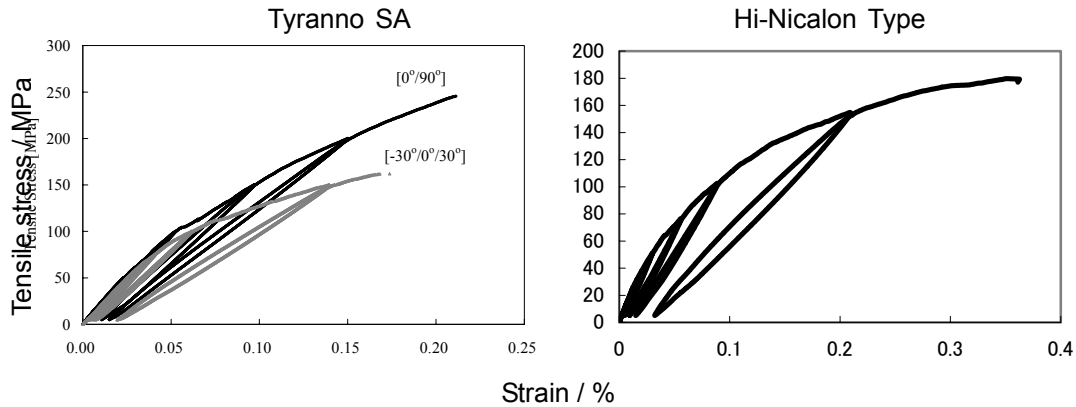


Fig. 8 Typical tensile behaviors of [-30°/0°/30°] and [0°/90°] SiC/SiC composites

Table 6. Mechanical properties of F-CVI SiC/SiC composites

Specimen ID	Tensile strength /MPa	Normalized tensile strength / MPa	Strain at fracture / %
CVI1256	155 ± 24	144 ± 22	0.126 ± 0.07
CVI1257	165 ± 23	164 ± 27	0.256 ± 0.15
CVI1258	164 ± 19	158 ± 18	0.204 ± 0.11
CVI1259	203 ± 10	201 ± 10	0.361 ± 0.05
CVI1260	131 ± 11	149 ± 12	0.173 ± 0.05
CVI1261	128 ± 19	133 ± 19	0.135 ± 0.03
CVI1264	233 ± 52	226 ± 33	0.253 ± 0.11
CVI1265	232 ± 34	226 ± 33	0.235 ± 0.03
CVI1266	211 ± 20	206 ± 20	0.175 ± 0.03

The composites fabricated by this study each have different density and fiber volume fraction. The relationship between the density of composite and the tensile strength is shown in Fig.9. No tendency can be, however, observed in this relationship. Because the load is mainly maintained by unfractured fibers and friction between fractured fiber and interphase above the proportional limit stress, the tensile strengths were, therefore, normalized by the fiber volume fraction of each composite in order to compare to them each other. Optimization of the interphase is one of the important

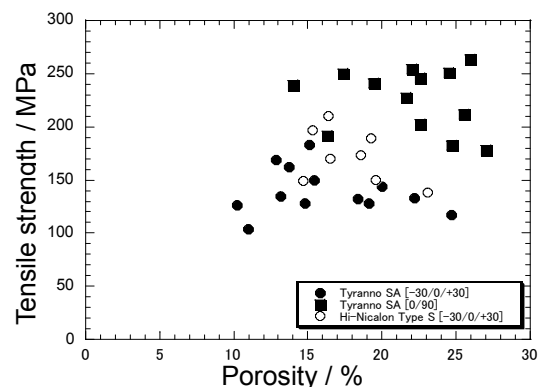


Fig.9 Effect of porosity on the tensile strength.

factors to improve the mechanical properties of SiC/SiC composites. The effect of carbon thickness on normalized tensile strength of SiC/SiC composites was shown in Fig.10. For the bend strength, the

optimum carbon interphase thickness is in the range of 170-1000nm[9]. In both $[0^\circ/90^\circ]$ and $[-30^\circ/0^\circ/30^\circ]$ composites using Tyranno SA fiber, it seems that normalized tensile strength is slightly increased with the thickness of carbon interphase in the range of 75-150 nm and then almost constant in the range of 150-300 nm. And in the composite using Hi-Nicalon Type S fiber, the normalized tensile strength was slightly increased with the thickness of carbon interphase in the range of 75-300 nm. The thick carbon layer as an interphase layer may cause the reduction of the strength in the composite following the neutron irradiation due to the irradiation-assisted oxidation and dimensional changes of the carbon [10,11]. The thinner carbon should be used as an interphase layer. From these results, the best thickness of carbon as an interphase layer may be about 150 nm.

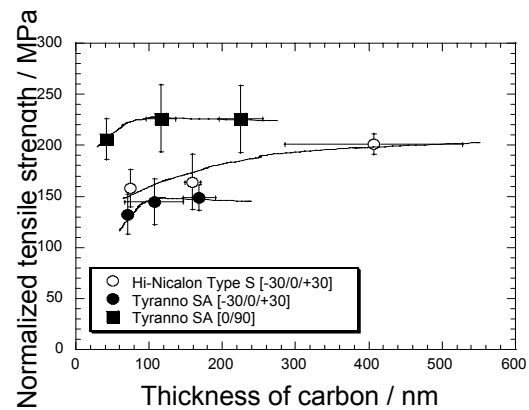


Fig.10 Effect of carbon thickness on the normalized tensile strength.

The tensile strength of the composite with the fabric orientation of $[0/90]$ using Tyranno SA fiber is larger than that of $[-30^\circ/0^\circ/30^\circ]$. The tensile fracture surfaces of the composites were shown in Fig.11. For the excellent tensile strength, a large number of fibers retained at a maximum load are required as well as the fiber strength itself[12]. In Fig.11 the fiber pull-out was observed in the tensile fracture surface of all specimens. It seems that the pull-out length of the fibres angled to the tensile axis is shorter than that of the aligned fiber with the tensile axis in the $[-30^\circ/0^\circ/30^\circ]$ composite. So the angled fibers might be unable to keep the strength. It is considered that the tensile strength depends on the strength of the aligned fiber with the tensile axis efficiently. The aligned fiber volume fraction with the tensile axis in the $[0^\circ/90^\circ]$ composite is higher than that of $[-30^\circ/0^\circ/30^\circ]$ composite. The tensile strength of $[0^\circ/90^\circ]$ composite was, therefore, larger than that of $[-30^\circ/0^\circ/30^\circ]$ composite.

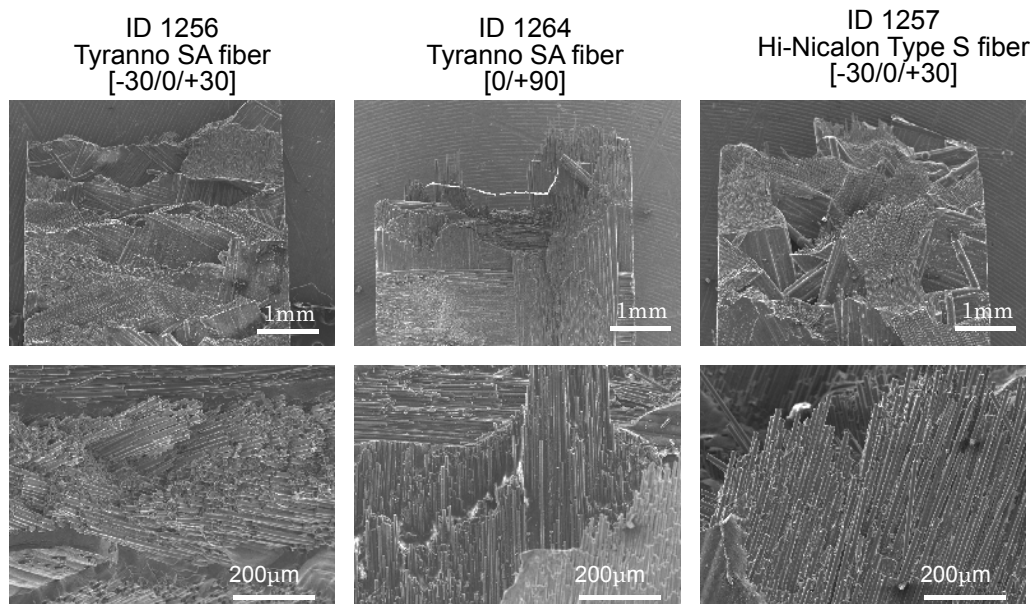


Fig.11 Fracture surface of tensile tested SiC/SiC composites with 150 nm carbon as an interphase layer.

In the case of fabric orientation of $[-30^\circ/0^\circ/30^\circ]$, the strength of the composite using Hi-Nicalon Type S is larger than that of Tyranno SA. From the result of the fracture surface observation (see Fig.11), it is found that the pull-out length of the composite using Hi-Nicalon Type S is longer than that of Tyranno SA. Especially the angled fibers with respect to the tensile axis also caused the long pull-out as well as the aligned fibers. It is considered that the angled fibers in the composite using Hi-Nicalon Type S could retain their strength. Therefore the strength of the composite using Hi-Nicalon Type S is larger than that of Tyranno SA.

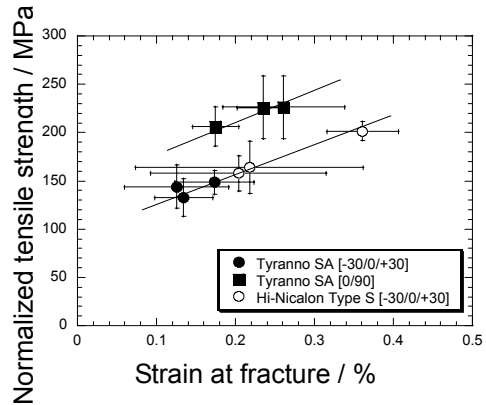


Fig.12 Relationship between strain and normalized tensile strength.

The normalized tensile strength as a function of the strain at tensile strength is shown in Fig.12. The normalized tensile strength increased linearly with increasing the strain. They depended on the fabric layer orientation but did not depend on the SiC fiber type. In the case of using Tyranno SA fiber, the strain of the composite with the fabric layer orientation of $[0^\circ/90^\circ]$ was larger than that of $[-30^\circ/0^\circ/30^\circ]$. The reason is that the aligned fiber volume fraction with the tensile axis in the $[0^\circ/90^\circ]$ composite is higher than that of $[-30^\circ/0^\circ/30^\circ]$ composite. In the case of fabric orientation of $[-30^\circ/0^\circ/30^\circ]$, the strain of the composite using Hi-Nicalon Type S is larger than that of Tyranno SA. As mentioned above, the reason is that the angled fibers also could cause the pull-out of composites using Hi-Nicalon Type S.

3.2 Fabrication of the 300 mm diameter composite

The 300 mm diameter size composites using the new SiC fiber with the optimized interphase will be fabricated. We fabricated the 300 mm diameter size composite using Nicalon fibers in order to estimate the carbon deposition rate on the new SiC fiber. The reason is that we can estimate the carbon deposition rate by that of other fiber type as mentioned in the previous section. The photograph of 300 mm diameter size SiC/SiC composite was shown in Fig.13. The fiber volume fraction is about 34.7 %. The density and porosity of this composite were about 2.57 g/cm^3 and 13.8 %, respectively. We are observing the cross-sections of this specimen by SEM to evaluate the thickness of carbon and SiC layer as the interphase.

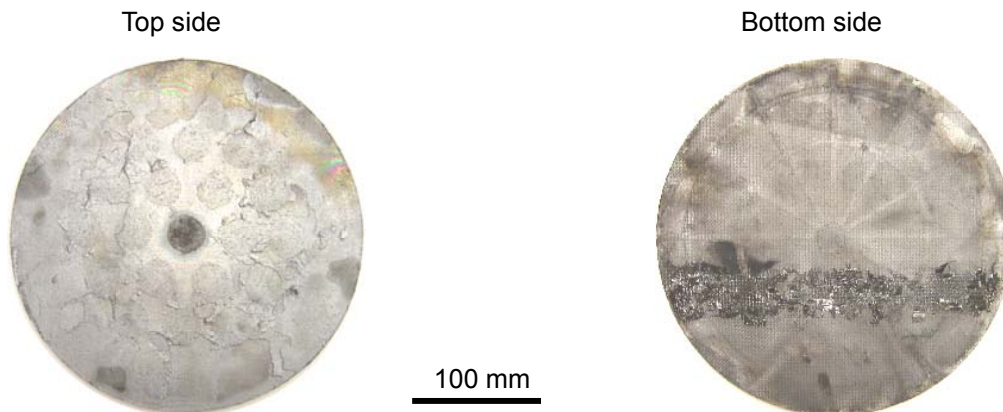


Fig.13 Photographs of the 300 mm diameter SiC/SiC composite using Nicalon fibers.

4. Conclusion

Process optimization for FCVI fabrication of 75 mm diameter SiC composites with new SiC fibers, Hi-Nicalon Type S and Tyranno SA, was carried out. The SiC/SiC composites fabricated by FCVI exhibited significant improvement reduction in porosity (15.1%) and more uniform pore distribution by decreasing in the MTS and H₂ gases flow rates at the latter part of the FCVI process. Uniform carbon interphase between advanced SiC fibers and FCVI-SiC matrix could be obtained by reversing the gas-flow direction mid-way through the coating process. The tensile strength was slightly increased with thickness of carbon interphase in the range of 75-300 nm.

From these results, the dense 300 mm diameter SiC/SiC composite using Nicalon fiber as a trial experiment was fabricated. The density and porosity were 2.57 g/cm³ and 13.8 %, respectively.

Acknowledgements

The authors would like to thank Dr. T. M. Besmann at ORNL for useful discussion. This study has been carried out under the US-DOE/ JAERI Collaborative Program on FWB Structural materials in Mixed-Spectrum Fission Reactors, Phase IV. This study is also supported by CREST-ACE(Core Research for Evolutional Science and Technology/Advanced material Systems for Energy Conversion) program sponsored by Japan Science and Technology Corporation.

References

- [1] L.L. Snead, R.H. Jones, A. Kohyama, P. Fenici, J. Nucl. Mater. 233-237(1996)26.
- [2] R.H. Jones, D. Steiner, H.L. Heinisch, G.A. Newsome, H.M. Kerch, J. Nucl. Mater.,245(1997)87.
- [3] P. Fenici, A.J. Frias Rebelo, R. H.Jones, A. Kohyama, L.L. Snead, J. Nucl. Mater. 258-263(1998)215.
- [4] A. Hasegawa, A. Kohyama, R.H. Jones, L.L. Snead, B. Riccardi, P. Fenici, J. Nucl. Mater. 283-287(2000)128.
- [5] T.M. Besmann, J.C. McLaughlin, H-T. Lin, J. Nucl. Mater. 219(1995)31.
- [6] M. Takeda, A. Urano, J. Sakamoto, Y. Imai, J. Nucl. Mater. 258-263(1998)1594.
- [7] T.Ishikawa, Y. Kohtoku, K. Kumagawa, T Yamamura, T. Nagasawa, Nature 391(1998)773..
- [8] W.S. Stefier, Ceram. Eng. Sci. Proc. 14(1993)1045.
- [9] A. Kohyama, H. Hinoki, H. Serizawa, S. Sato, Proc. of 11th Inter. Conf. on Composites Mater. 1997.
- [10] L.L.Snead, M.C.Osborne and K.L.More, J. Nucl. Mater., 231 (1996) 245-248.
- [11] J.H.W.Simmons, Radiation Damage in Graphite, Pergamon Press, (1965).
- [12] T. Hinoki, W. Yang, T. Nozawa, T. Shibayama, Y. Katoh, A. Kohyama, J. Nucl. Mater. 289(2001)23.